A General Approach for Synthesizing Multibeam Antenna Arrays Employing Generalized Joined Coupler Matrix

Charles A. Guo, *Student Member, IEEE,* and Y. Guo, *Fellow, IEEE*

***Abstract*—Despite the rapidly increasing interest in analogue multibeam antennas, there has been a lack of systematic theoretical approaches to synthesizing circuit-type multiple beamforming networks, such as the Blass matrix and the Nolen matrix. To address the issue, this paper presents a new concept, Generalised Joined Coupler (GJC) matrix, which encapsulates both the Blass matrix and the Nolen matrix as well as their variants, and presents a novel theoretical framework for generating *individually* and *independently controllable* multiple beams using the GJC matrix. A GJC matrix has N columns to feed N antenna elements and M rows to feed M beams, and the direction of each individual beam can be controlled by tuning the phase shifters in the associated row of the GJC matrix. In the paper, a matrix theory is developed and an optimization algorithm is proposed to provide a mathematical tool for synthesizing such matrices and consequently the multiple beams. Using a particle swarm optimization algorithm, numerical results demonstrate that multibeams with independent control of individual beam directions and sidelobes can indeed be synthesized in a systematic manner. Specifically, two GJC matrix variants, the Blass-like matrix and the Nolen-like matrix are investigated.**

***Index Terms*—Blass matrix, Blass-like matrix, Feed networks, GJC matrix, Individual beam control, Low sidelobes, Multibeam phased arrays, Nolen matrix, Nolen-like matrix.**

I. Introduction

MULTIBEAM antennas are regarded as a critical technology for 5G and beyond 5G (B5G) wireless communications networks [1], [2], [3]. In comparison to digital beamforming techniques, analogue beamforming techniques are of low cost and low energy consumption [4]. Analogue multibeams can be formed by using either circuit-type feed networks or quasi-optical approaches [5]. Widely known circuit-type feed networks for feeding multibeam antennas include the Butler matrix, the Blass matrix and the Nolen matrix [1], [4]. The standard Butler matrix is an $N \times N$ square matrix using hybrid couplers to produce N orthogonal beams. Although all the beams can be rotated together, their relative directions are fixed. Therefore, the Butler matrix is most suited for covering sectors in conventional base stations. Since its inception [6], a large number of papers have been published on the Butler matrix. These include systematic design approaches [7] and various innovative designs such as wideband and low sidelobe beam realizations [1], [8]. Unlike Butler matrices, Blass matrices and Nolen matrices employ directional couplers and phase shifters without crossovers to produce flexible multibeams which can be designed to point in desired directions [9], [10]. A Blass matrix is an $M \times N (M \leq N)$ rectangular matrix with matched loads at the end of each row and column to produce M beams, thus making it lossy. A Nolen matrix is an $N \times N$ diagonal matrix with the nodes lying along the diagonal constructed to direct all ingoing energy to the row above, hence making it lossless and also saving almost half of the matrix nodes. Although the general thinking is that such matrix savings in nodes and circuit components in the Nolen matrix are advantageous, as we show in this paper, this may result in the degradation of the beamforming performance.

Beamforming networks such as Blass and Nolen matrices have two functions. The first function is to route different input signals to the antenna elements to realize desired signal magnitude distributions across the antenna array. The second function is to produce different phase distributions to realize desired beam directions for different input signals. The major building blocks of these matrices are joined couplers that consist of a number of directional couplers joined together to perform the task of signal routing. A chief task in synthesizing Blass and Nolen matrices is to determine the parameters of the joined couplers. To treat all these matrices in a universal manner, therefore, we introduce a new concept, the generalised joined coupler (GJC) matrix, which encompasses the Blass matrix, the Nolen matrix and other variants. A particularly interesting new variant of the GJC matrix is also introduced in this paper, in which the phase shifter associated with each matrix node is placed to the right of the directional coupler instead of above it as is the case in conventional matrices. This makes it possible to realise *independent* individual beam scanning. A salient feature of GJC matrices is that they can be used to produce up to N number of beams flexibly by adjusting the number of matrix nodes required, the coupling coefficients, the associated phase shifter of each node, and the termination of the matrix. Driven by multiuser communications and peer-to-peer networking, the interest in GJC matrices is expected to grow in order to meet the demands of future wireless communications such as 5G, B5G and 6G systems [1] - [4].

One of the primary difficulties in employing Blass matrices or Nolen matrices, and GJC matrices in general, is the complexity of synthesizing the matrix. This is in contrast to the Butler matrix; the methods for designing it have been

Charles A. Guo is with the School of Electrical Engineering and Telecommunications, University of New South Wales, NSW2052, Australia (email: z5280551@ad.unsw.edu.au).

Y. Guo is with the Global Big Data Technologies Centre, University of Technology Sydney, NSW 2007, Australia (email: jay.guo@uts.edu.au).

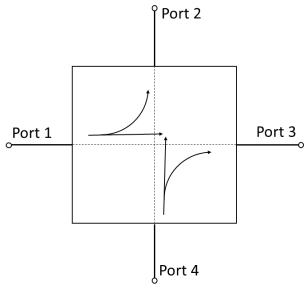

Fig. 1: Illustration of the functionality of a directional coupler.

well developed [7], [11]. Some design procedures for special Blass matrices and Nolen matrices have been reported in the literature. In [12], a method was proposed for a matrix with a maximum of two rows, and the procedures shown in [13], [14] do not allow users to arbitrarily choose the position of the generated beams. What was presented in [15] is a non-systematic path-by-path approach. More recently, closed-form equations for a uniplanar single 3×3 Nolen matrix were reported in [16]. Owing to the lack of systematic theoretical work on the topic, there have been scant publications investigating the synthesis of multiple beams and their individual control in spite of the increasing interest from the antenna and microwave communities [17], [18], [19].

In this paper, we present a novel systematic approach for synthesizing flexible multibeams employing GJC matrices. In Section II, a matrix form expression linking the GJC matrix outputs, i.e., the antenna excitation coefficients, with the array input ports or beam ports is derived first. This not only provides a mathematical framework for multibeam synthesis, but also enables us to reveal various characteristics of the Blass matrix and the Nolen matrix for the first time. In Section III, we propose a computationally efficient optimization method to synthesise a GJC matrix in order to generate desired multibeams. In Section IV, we present some examples of synthesizing multiple beams using Blass-like and Nolen-like GJC matrices, and reveal some features of these systems including beam scanning and the realization of low sidelobe beam patterns. Section V concludes the paper.

II. Theoretical Framework

To feed a single beam antenna array, one needs a number of power dividers and phase shifters to produce the desired array excitation coefficients [20]. For convenience, we shall refer to a set of such coefficients as an *array excitation vector*. In order to produce flexible multibeams, one would need a GJC matrix. The directional couplers in the GJC matrix are used for directing the signal flow and distribution, and the phase shifters are needed to produce beams in different directions. In general, the function of a directional coupler can be illustrated in Fig. 1. The ports are indexed clockwise. The signal transfer among the four ports is described by an $\boldsymbol{S}$ matrix given by [21]:

$$\boldsymbol{S} = \begin{bmatrix} 0 & j\sin\theta & \cos\theta & 0 \\ j\sin\theta & 0 & 0 & \cos\theta \\ \cos\theta & 0 & 0 & j\sin\theta \\ 0 & \cos\theta & j\sin\theta & 0 \end{bmatrix}, \tag{1}$$

where $j = \sqrt{-1}$. As shown in Fig. 2, a GJC matrix consists of directional couplers and phase shifters. A directional coupler and a phase shifter comprise a matrix node as shown in Fig. 3. For a GJC matrix, we use m to represent the m^{th} row corresponding to the m^{th} input signal, and n the order of the n^{th} column corresponding to the n^{th} antenna element. We denote θ_{mn} as the parameter for determining the signal flow within a directional coupler in the node positioned in the m^{th} row and the n^{th} column of a GJC matrix, and φ_{mn} the phase shifter value of this same node. It must be noted that, in Fig. 2, the phase shifter in each matrix node is connected to port 3 of its corresponding directional coupler, whereas in traditional Blass matrices and Nolen matrices, each phase shifter is connected to port 2 of its corresponding directional coupler. This important difference makes it possible to realise independent individual beam scanning. In Fig. 2, there are four antenna input ports with input x_m, $m = 1,\ 2,\ 3,\ 4$, and the array excitation vector is given by y_n, $n = 1,\ 2,\ \ldots,\ N$ with N representing the number of antenna elements. In what follows, the signal inputs x_m are collectively referred to as the *array input vector*.

Owing to the use of directional couplers, the signal flowing through any antenna port or beam port to the inside of the GJC matrix only travels upwards and to the right, as shown in Fig. 1, with its $\boldsymbol{S}$ matrix in (1). The lower the antenna input port, the more paths the signal flow takes. This makes the handling of GJC matrices with more than two rows highly complex. Few approaches have been proposed in the past to find the general relationship between the array input vector and the array excitation vector. Such lack of a general theory may partly explain the slow uptake of Blass and Nolen matrices for creating multibeams. In the following, we take a matrix approach to derive their relationship in a closed form formula for the first time.

Given that the matrix shown in Fig. 2 is a cascade of a number of similar vertical units, or columns, each consisting of four directional couplers and four phase shifters, or a conjunction of four nodes. For the n^{th} column, one can express the relationship between their inputs and horizontal outputs as follows:

$$\begin{aligned} u_{1n} = \cos\theta_{1n}\ e^{-j\varphi_1} u_{1(n-1)} + j^2\sin\theta_{1n}\ \sin\theta_{2n}\ e^{-j\varphi_{1n}} u_{2(n-1)} + j^2\sin\theta_{1n}\ \cos\theta_{2n}\ \sin\theta_{3n}\ e^{-j\varphi_{1n}} u_{3(n-1)} \\ + j^2\sin\theta_{1n}\ \cos\theta_{2n}\ \cos\theta_{3n}\ \sin\theta_{4n}\ e^{-j\varphi_{1n}} u_{4(n-1)}, \end{aligned} \tag{2a}$$

$$u_{2n} = \cos\theta_{2n}\ e^{-j\varphi_{2n}} u_{2(n-1)} + j^2\sin\theta_{2n}\ \sin\theta_{3n}\ e^{-j\varphi_{2n}} u_{3(n-1)} + j^2\sin\theta_{2n}\ \cos\theta_{3n}\ \sin\theta_{4n}\ e^{-j\varphi_{2n}} u_{4(n-1)}, \tag{2b}$$

$$u_{3n} = \cos\theta_{3n}\ e^{-j\varphi_{3n}} u_{3(n-1)} + j^2\sin\theta_{3n}\ \sin\theta_{4n}\ e^{-j\varphi_{3n}} u_{4(n-1)}, \tag{2c}$$

$$u_{4n} = \cos\theta_{4n}\ e^{-j\varphi_{4n}} u_{4(n-1)}. \tag{2d}$$

Without loss of generality N is chosen as 4 first. In (2a), (2b), (2c), and (2d), the first subscript, e.g. 1 and 2 in u_{1n} and u_{2n}, are aligned with the order of the nodes (see Fig. 2). The second subscript, such as n in u_{1n} and u_{2n}, represents the position of the column. As indicated by the number of terms in each equation, (2d), (2c), (2b), and (2a) show that only one signal travels through the bottom node and progressively more signals go through the upper nodes.

Defining the signal transformation matrix of the n^{th} column as:

$$\boldsymbol{A}_{4\times4}^{(n)} = \begin{bmatrix} cos\theta_{1n}\ e^{-j\varphi_{1n}} & j^2 sin\theta_{1n}\ sin\theta_{2n}\ e^{-j\varphi_{1n}} & j^2 sin\theta_{1n}\ cos\theta_{2n}\ sin\theta_{3n}\ e^{-j\varphi_{1n}} & j^2 sin\theta_{1n}\ cos\theta_{2n}\ cos\theta_{3n}\ sin\theta_{4n}\ e^{-j\varphi_{1n}} \\ 0 & cos\theta_{2n}\ e^{-j\varphi_{2n}} & j^2 sin\theta_{2n}\ sin\theta_{3n}\ e^{-j\varphi_{2n}} & j^2 sin\theta_{2n}\ cos\theta_{3n}\ sin\theta_{4n}\ e^{-j\varphi_{2n}} \\ 0 & 0 & cos\theta_{3n}\ e^{-j\varphi_{3n}} & j^2 sin\theta_{3n}\ sin\theta_{4n}\ e^{-j\varphi_{3n}} \\ 0 & 0 & 0 & cos\theta_{4n}\ e^{-j\varphi_{4n}} \end{bmatrix}_{4\times4}, \tag{3}$$

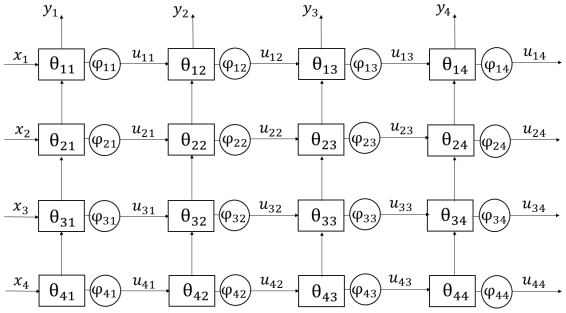

Fig. 2: Part of a GJC matrix for transmitting four beams.

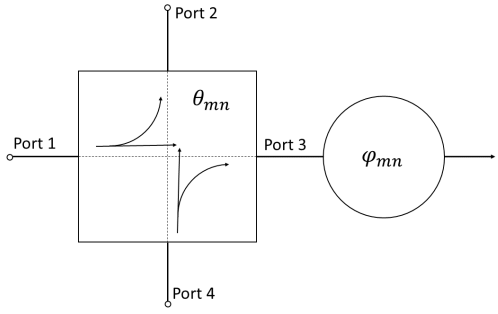

Fig. 3: A directional coupler and a phase shifter form a GJC matrix node.

The signals entering horizontally into the first column of the GJC matrix are transformed to the output as:

$$\begin{bmatrix} u_{11} \\ u_{21} \\ u_{31} \\ u_{41} \end{bmatrix} = \boldsymbol{A}_{4\times4}^{(1)} \begin{bmatrix} x_1 \\ x_2 \\ x_3 \\ x_4 \end{bmatrix}, \tag{4a}$$

and the signal transformation taking place at the n^{th} column of the GJC matrix is described as:

$$\begin{bmatrix} u_{1n} \\ u_{2n} \\ u_{3n} \\ u_{4n} \end{bmatrix} = \boldsymbol{A}_{4\times4}^{(n)} \begin{bmatrix} u_{1(n-1)} \\ u_{2(n-1)} \\ u_{3(n-1)} \\ u_{4(n-1)} \end{bmatrix}, \tag{4b}$$

$$2 \leq n \leq 4.$$

More specifically, one has:

$$\begin{bmatrix} u_{12} \\ u_{22} \\ u_{32} \\ u_{42} \end{bmatrix} = \boldsymbol{A}_{4\times4}^{(2)} \begin{bmatrix} u_{11} \\ u_{21} \\ u_{31} \\ u_{41} \end{bmatrix} = \boldsymbol{A}_{4\times4}^{(2)} \boldsymbol{A}_{4\times4}^{(1)} \begin{bmatrix} x_1 \\ x_2 \\ x_3 \\ x_4 \end{bmatrix}, \tag{4c}$$

$$\begin{bmatrix} u_{13} \\ u_{23} \\ u_{33} \\ u_{43} \end{bmatrix} = \boldsymbol{A}_{4\times4}^{(3)} \boldsymbol{A}_{4\times4}^{(2)} \boldsymbol{A}_{4\times4}^{(1)} \begin{bmatrix} x_1 \\ x_2 \\ x_3 \\ x_4 \end{bmatrix}, \tag{4d}$$

$$\begin{bmatrix} u_{14} \\ u_{24} \\ u_{34} \\ u_{44} \end{bmatrix} = \boldsymbol{A}_{4\times4}^{(4)} \boldsymbol{A}_{4\times4}^{(3)} \boldsymbol{A}_{4\times4}^{(2)} \boldsymbol{A}_{4\times4}^{(1)} \begin{bmatrix} x_1 \\ x_2 \\ x_3 \\ x_4 \end{bmatrix}. \tag{4e}$$

Note that a signal passing through a directional coupler can continue horizontally or can be directed upwards as shown in Fig. 1. The transformation of the signals in the first column of a GJC matrix that are directed towards the first antenna is represented as:

$$y_1 = \left[\boldsymbol{\alpha}_{4\times1}^{(1)}\right]^T \begin{bmatrix} x_1 \\ x_2 \\ x_3 \\ x_4 \end{bmatrix}, \tag{5a}$$

where:

$$\boldsymbol{\alpha}_{4\times1}^{(1)} = \begin{bmatrix} j\sin\theta_{11} \\ j\sin\theta_{21}\ \cos\theta_{11} \\ j\sin\theta_{31}\ \cos\theta_{21}\ \cos\theta_{11} \\ j\sin\theta_{41}\ \cos\theta_{31}\ \cos\theta_{21}\ \cos\theta_{11} \end{bmatrix}_{4\times1}. \tag{5b}$$

The transformation of signals in the n^{th} column of the GJC matrix that are directed towards the n^{th} antenna is represented as:

$$y_n = \left[\boldsymbol{\alpha}_{4\times1}^{(n)}\right]^T \begin{bmatrix} u_{1(n-1)} \\ u_{2(n-1)} \\ u_{3(n-1)} \\ u_{4(n-1)} \end{bmatrix}, \tag{5c}$$

where:

$$\boldsymbol{\alpha}_{4\times1}^{(n)} = \begin{bmatrix} j\sin\theta_{1n} \\ j\sin\theta_{2n}\ \cos\theta_{1n} \\ j\sin\theta_{3n}\ \cos\theta_{2n}\ \cos\theta_{1n} \\ j\sin\theta_{4n}\ \cos\theta_{3n}\ \cos\theta_{2n}\ \cos\theta_{1n} \end{bmatrix}_{4\times1}. \tag{5d}$$

Consequently, we have the following expression of the array excitation vector in terms of the array input vector:

$$\begin{bmatrix} y_1 \\ y_2 \\ y_3 \\ y_4 \end{bmatrix} = \boldsymbol{\Omega}_{4\times4} \begin{bmatrix} x_1 \\ x_2 \\ x_3 \\ x_4 \end{bmatrix}, \tag{5e}$$

where:

$$\boldsymbol{\Omega}_{4\times4} = \begin{bmatrix} \left[\boldsymbol{\alpha}_{4\times1}^{(1)}\right]^T \\ \left[\boldsymbol{\alpha}_{4\times1}^{(2)}\right]^T \boldsymbol{A}_{4\times4}^{(1)} \\ \left[\boldsymbol{\alpha}_{4\times1}^{(3)}\right]^T \boldsymbol{A}_{4\times4}^{(2)}\boldsymbol{A}_{4\times4}^{(1)} \\ \left[\boldsymbol{\alpha}_{4\times1}^{(4)}\right]^T \boldsymbol{A}_{4\times4}^{(3)}\boldsymbol{A}_{4\times4}^{(2)}\boldsymbol{A}_{4\times4}^{(1)} \end{bmatrix}_{4\times4}. \tag{5f}$$

The above derivation is for a full GJC matrix with four antenna input ports and four antenna elements, and the antenna excitation vector is $[y_1, y_2, y_3, y_4]^T$.

A general full GJC matrix with M signal input ports and N antenna elements to feed is shown in Fig. 4. All the major matrices for the general case are derived following the above procedure, and are given below.

We define the general signal transformation matrix for the n^{th} column of a GJC matrix as:

$$\boldsymbol{A}_{M\times M}^{(n)} = \begin{bmatrix} cos\theta_{1n}\ e^{-j\varphi_{1n}} & j^2 sin\theta_{1n}\ sin\theta_{2n}\ e^{-j\varphi_{1n}} & \cdots & j^2 sin\theta_1 n\ cos\theta_{2n} \ldots cos\theta_{(M-1)n}\ sin\theta_{Mn}\ e^{-j\varphi_{1n}} \\ 0 & cos\theta_{2n}\ e^{-j\varphi_{2n}} & \cdots & j^2 sin\theta_{2n}\ cos\theta_{3n}\ \ldots cos\theta_{(M-1)n}\ sin\theta_{Mn}\ e^{-j\varphi_{2n}} \\ 0 & 0 & \cdots & j^2 sin\theta_{3n}\ cos\theta_{4n}\ \ldots cos\theta_{(M-1)n}\ sin\theta_{Mn}\ e^{-j\varphi_{3n}} \\ \vdots & \vdots & \ddots & \vdots \\ 0 & 0 & \cdots & cos\theta_{Mn}\ e^{-j\varphi_{Mn}} \end{bmatrix}_{M\times M}, \tag{6}$$

where the superscript of $\boldsymbol{A}_{M\times M}^{(n)}$ describes the n^{th} column of the GJC matrix transformation. The signals passing horizontally through the first column of joined couplers are transformed as:

$$\begin{bmatrix} u_{11} \\ u_{21} \\ \vdots \\ u_{M1} \end{bmatrix} = \boldsymbol{A}_{M\times M}^{(1)} \begin{bmatrix} x_1 \\ x_2 \\ \vdots \\ x_M \end{bmatrix}, \tag{7}$$

and that through the n^{th} column of joined couplers as:

$$\begin{bmatrix} u_{1n} \\ u_{2n} \\ \vdots \\ u_{Mn} \end{bmatrix} = \boldsymbol{A}_{M\times M}^{(n)} \begin{bmatrix} u_{1(n-1)} \\ u_{2(n-1)} \\ \vdots \\ u_{M(n-1)} \end{bmatrix}, \tag{8}$$

$$2 \le n \le N.$$

Defining:

$$\boldsymbol{\alpha}_{M\times1}^{(n)} = \begin{bmatrix} j\sin\theta_{1n} \\ j\sin\theta_{2n}\ \cos\theta_{1n} \\ j\sin\theta_{3n}\ \cos\theta_{2n}\ \cos\theta_{1n} \\ \vdots \\ j\sin\theta_{Mn}\ \cos\theta_{(M-1)n}\ \cos\theta_{(M-2)n}\ \cdots\cos\theta_{1n} \end{bmatrix}_{M\times1}, \tag{9}$$

the transformation of the signals in the first column of the GJC matrix that are directed towards the first antenna is represented as:

$$y_1 = \left[\boldsymbol{\alpha}_{M\times1}^{(1)}\right]^T \begin{bmatrix} x_1 \\ x_2 \\ x_3 \\ \vdots \\ x_M \end{bmatrix}, \tag{10}$$

and that directed by the n^{th} column of the GJC matrix to the n^{th} antenna is:

$$y_n = \left[\boldsymbol{\alpha}_{M\times1}^{(n)}\right]^T \begin{bmatrix} u_{1(n-1)} \\ u_{2(n-1)} \\ u_{3(n-1)} \\ \vdots \\ u_{M(n-1)} \end{bmatrix}. \tag{11}$$

Combining (6), (7), (8), (9), (10), and (11) yields:

$$\begin{bmatrix} y_1 \\ y_2 \\ \vdots \\ y_n \\ \vdots \\ y_N \end{bmatrix} = \boldsymbol{\Omega}_{N\times M} \begin{bmatrix} x_1 \\ x_2 \\ \vdots \\ x_M \end{bmatrix}, \tag{12}$$

where:

$$\boldsymbol{\Omega}_{N\times M} = \begin{bmatrix} \left[\boldsymbol{\alpha}^{(1)}_{M\times 1}\right]^T \\ \left[\boldsymbol{\alpha}^{(2)}_{M\times 1}\right]^T \boldsymbol{A}^{(1)}_{M\times M} \\ \vdots \\ \left[\boldsymbol{\alpha}^{(n)}_{M\times 1}\right]^T \boldsymbol{A}^{(n-1)}_{M\times M}\cdots \boldsymbol{A}^{(1)}{}_{M\times M} \\ \vdots \\ \left[\boldsymbol{\alpha}^{(N)}_{M\times 1}\right]^T \boldsymbol{A}^{(N-1)}_{M\times M}\cdots \boldsymbol{A}^{(1)}{}_{M\times M} \end{bmatrix}_{N\times M}. \quad (13)$$

To quantify the losses occurring in the matched loads, we define the *transmission efficiency* of the GJC matrix as:

$$\eta_t = 1 - \sum_{n}^{M} u_{nN}^2 / \sum_{i}^{M} x_n^2. \quad (14)$$

It should be noted that the transmission efficiency of the GJC matrix defined in (14) is for all of the beams, but it can also be used to calculate the transmission efficiency of individual beams. It is a representation of how much ohmic loss occurs in the matrix. In the case of the Blass matrix, the losses will occur in the matched loads at the end of each row and column. In the case of the Nolen matrix, the transmission efficiency is theoretically 100% if all of the matrix nodes are lossless. In the case of a general GJC matrix where some nodes are connected to a matched load and some may be treated in the same way as in the Nolen matrix, (14) can be easily modified to calculate the transmission efficiency.

With the above equations, one can obtain the antenna excitation vector of any antenna beam by considering only one beam input at a time. In practice, we would be faced with the problem of synthesizing multibeams by synthesizing the GJC matrix. This will be discussed in the next section.

III. Design of GJC Matrices for Multiple Beams

The synthesis of single beam arrays is usually treated as a problem of optimizing the antenna weights, or the array excitation vector. Similarly, the synthesis of multiple beams can be treated as a problem of optimizing the parameters of a GJC matrix to produce M predefined beams. There is a wealth of literature on single antenna pattern synthesis using optimization methods [22]. Typically, one would need to calculate the radiation pattern in an angular range of interest in each optimization step, and use a cost function to guide the iteration process in order to obtain the optimal array excitation vector to achieve the desired beam pattern. This can be computationally time-consuming for producing multibeams, especially when the dimensions of the GJC matrix are large. In the following, we propose to synthesize GJC matrices by optimizing the array excitation vector for each beam directly. This is much more computationally efficient as one can use a classical array distribution function such as the uniform, Taylor, or Chebyshev distributions as the targeted array excitation vectors [20]; no beam pattern calculation is required. Thanks to the employment of the phase shifters in each row of the GJC matrix, no optimization of the phase distribution is required in the proposed strategy.

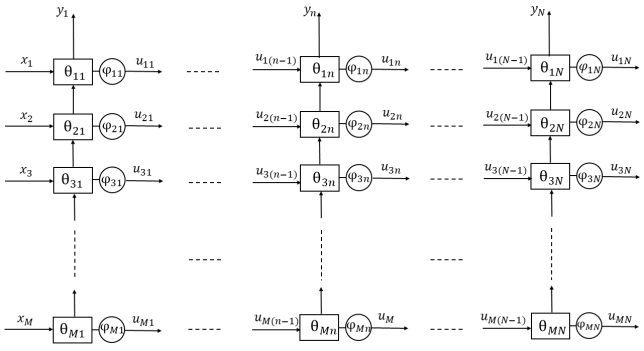

Fig. 4: Part of a general GJC matrix.

A. Single Beam Synthesis

We first start with the synthesis of a single beam. This is equivalent to synthesizing a series-fed linear antenna array or a leaky wave antenna. This special case is pertinent because it can be used as the first step in synthesizing multibeams. We choose to optimize the GJC matrix to produce a uniform array excitation to produce the sharpest antenna beam with maximum aperture efficiency. Intuitively, the power "leakage" should be as $[\ 1/N, 1/\left(N-1\right), 1/\left(N-2\right),\ \ldots, 1\ ]$, where N is the number of antenna elements. The coupler parameter θ_{1n} $(n = 1,\ 2,\ \ldots,\ N)$ is thus given by:

$$\theta_{1n} = \sin^{-1}\frac{1}{\sqrt{N-n+1}}, \quad (15)$$

which results in a uniform array excitation. A constant phase shift φ_1 can be assigned to produce a beam in the following direction:

$$\gamma_1 = \sin^{-1}\frac{\varphi_1}{kd}, \quad (16)$$

where k is the wavenumber and d is the antenna element spacing; a uniformly distanced array has been assumed. It should be noted that, if we use the above approach, the feed network is lossless, as all the input energy is radiated. This is important as (15) can be used to design series fed liner antenna arrays and leaky wave antennas. An alternative approach is to synthesize beam 1 in the same way as other beams.

B. Multibeam Synthesis

Next, we show how to synthesize multiple beams. We can keep the directional coupler and phase shifter design for beam 1 the same as in (15) and (16) above, and then synthesize the couplers in the other rows of the GJC matrix (see Fig. 2). Intuitively, we can keep all the phase shifts the same as φ_2 to obtain the second beam in the direction of γ_2 as follows:

$$\gamma_2 = \sin^{-1}\frac{\varphi_2}{kd}. \quad (17)$$

This is where the complexity of the problem arises. Since the signal flow from the second row to the first row of the GJC matrix and then to the antennas takes place via many

different multi-paths, we no longer know how to set the coupler parameters optimally to obtain a desired beam pattern as for the first beam. Furthermore, we typically need to keep the transmission efficiency high. Therefore, we need to resort to an optimization strategy.

From beam 2 onwards, we define the targeted magnitude distribution of the array excitation vector elements for the m^{th} beam as $Y_n^{(m)}$, $n = 1,\ 2,\ \cdots,\ N$. $Y_n^{(m)}$, $n = 1,\ 2,\ \cdots,\ N$ can be chosen from a classic distribution such as the uniform distribution or the Taylor distribution. Then, the cost function for the optimization of the couplers in the m^{th} row of the GJC matrix is given by:

$$f^{(m)}(\boldsymbol{\theta}^{(m)}) = \sum_{n=1}^{N} \left| \left| y_n^{(m)}(\boldsymbol{\theta}^{(m)}) \right| - Y_n^{(m)} \right|, \tag{18}$$

$$\gamma_m = \sin^{-1} \frac{\varphi_m}{kd}, \tag{19}$$

where $y_n^{(m)}$, $n = 1,\ 2,\ \ldots,\ N$ are the antenna excitations generated by the GJC matrix for the m^{th} beam based on (11). In practice, we can make the magnitude distribution of all the targeted array excitation vectors the same. It should be noted that in (18) we have chosen to optimize the magnitudes of the array excitation vector elements. This is because the phases of these elements are determined by the phase shifter values given by (19). When implementing the uniform excitation, $Y_n^{(m)}$ can be calculated as:

$$Y_n^{(m)} = \frac{1}{\sqrt{N}}. \tag{20}$$

Our strategy is to optimize the coupler parameters $\theta_n^{(m)}$, $n = 1,\ 2,\ \ldots,\ N$ in order to minimize the cost function $f^{(m)}$. It is noted that the L_1 norm is employed in (18), though other norms can also be used. Successful synthesis of a desired beam is achieved in practice when the cost function reaches a minimum.

Thus, an algorithm for synthesizing multiple beams is given as follows:

Multibeam Synthesis Algorithm

1) Select the magnitude distribution of the antenna coefficients for the M beams;
2) Select the directions of M beams and set the phase shifter values using (19);
3) Define a cost function for optimization, such as the one given in (18);
4) Optimise the directional couplers in the first row of the GJC matrix using an optimization algorithm;
5) Use the above directional coupler values for the first row in the GJC matrix and then optimize the directional couplers in the second row of the GJC matrix;
6) Repeat step 5 until M beams have been synthesized.

Owing to the complexity of this form of objective functions, it has become a common practice to use Genetic Algorithm or Particle Swarm Optimization (PSO) algorithm for array synthesis [23]. In this paper, therefore, the PSO algorithm is employed.

IV. Numerical Examples

To verify the theory developed in Section II and the GJC matrix synthesis strategy proposed in Section III, we present some numerical results and reveal some characteristics of GJC matrices.

As stated in the introduction, GJC matrices have a number of variants. In what follows, we focus on those variants in which the phase shifters are placed to the right of the associated directional couplers. Specifically, we examine two important variants, namely, the Blass-like GJC matrix and the Nolen-like GJC matrix.

A. Multiple Beamforming and Sidelobe Control

We first demonstrate the effectiveness of the proposed approach in synthesizing Blass-like GJC matrices for generating multiple beams. The illustration of such a matrix is given in Fig. 5. To date, owing to the lack of accessible theoretical methods on the topic, there has been a scant number of publications investigating the use of Blass matrices to produce more than two beams, Fig. 6 shows three beam patterns of an 8-element array fed by a Blass-like GJC matrix with uniform distribution as the targeted magnitude distribution of the array excitation vector. The beams numbered as b1, b2 and b3 are pointed at ($-30°$, $0°$, $30°$) as intended in the matrix synthesis, with side lobes less than -12 dB. We can see that the proposed optimization strategy does result in desired results. The magnitude of the antenna excitation coefficients and the antenna efficiency are shown in Table I. To compare, Fig. 7 shows three beam patterns of a 12-element array fed by a Blass-like GJC matrix. The simulated beams are again pointed at ($-30°$, $0°$, $30°$) as intended in the synthesis. In this case, the transmission efficiency is increased from 95.8% to 97%. The magnitude of the antenna excitation coefficients and the GJC matrix transmission efficiency are shown in Table II. From these two examples, we observe that despite the conventional perception that Blass matrices are generally lossy and therefore would be undeserving of implementation, their transmission efficiency can actually be made high.

The beam patterns in Fig. 6 and Fig. 7 are obtained with uniform antenna excitation coefficients for all the beams. The leftmost beams are created by the first row of the GJC matrix and, as such, they exhibit classical linear array beam patterns. Because of the multipath effects, however, it is seen that the sidelobe levels of other beams, corresponding to beam ports that are lower in the GJC matrix, deteriorate. In practice, low sidelobe levels may be required for some or all of the beams. To achieve this, we can use tapered antenna excitations as the objective for optimization, such as the Taylor distribution or the Chebyshev distribution. Fig. 8 shows three beams created by using 20 antenna elements with a Taylor distribution exhibiting -20 dB sidelobe levels [20]. It is seen that, counting from the left, although the sidelobe levels of the second and third beams do increase from that of the first, they are still close to -20 dB. Fig. 9 shows the results of synthesizing five

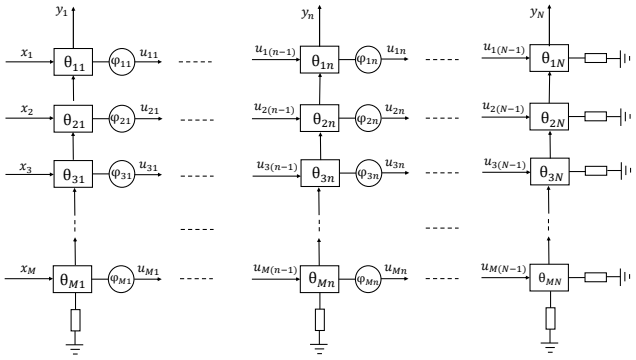

Fig. 5: Illustration of a Blass-like GJC matrix.

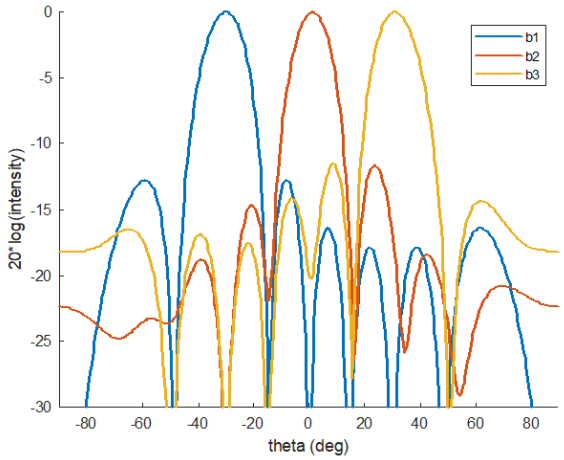

Fig. 6: Synthesized beam patterns using a Blass matrix when $M = 3$, and $N = 8$.

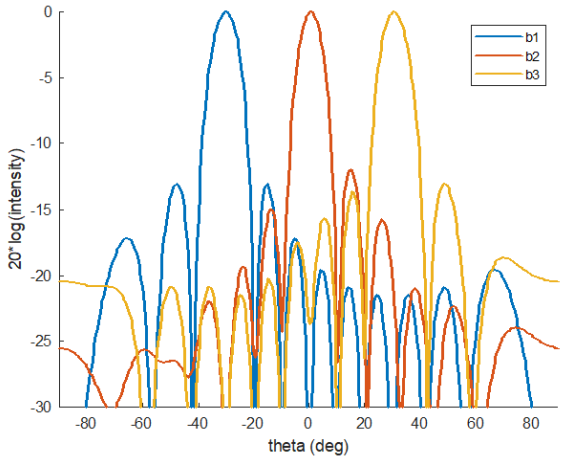

Fig. 7: Synthesized beam patterns using a Blass matrix when $M = 3$, and $N = 12$.

beams using the same amplitude taper, and it is seen that the sidelobe levels of the third to fifth beams have increased to -15 dB. This demonstrates that the multi-path effect does become stronger as the beam number increases.

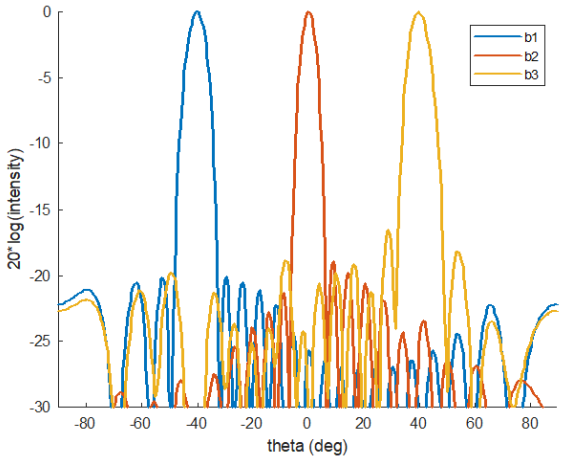

Fig. 8: Three beams produced by using 20 antenna elements and a Taylor distribution (M=3, N=20).

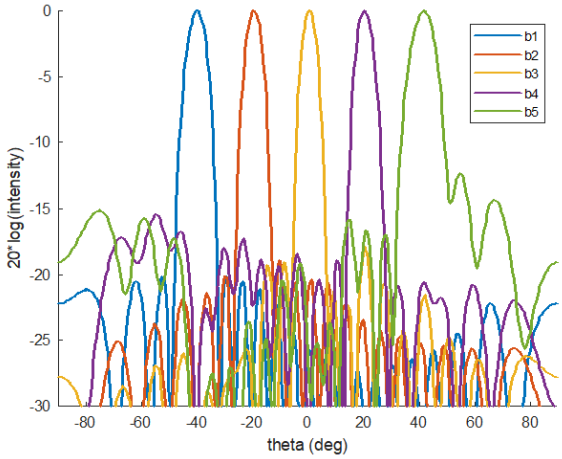

Fig. 9: Five beams produced by using 20 antenna elements and a Taylor distribution (M=5, N=20).

B. Beam Scanning

The single row matrix presented in Section III-A can be used to produce a scanning beam by simply changing the phase shift values and optimizing the directional coupler parameters to obtain the desired antenna excitation coefficients. It is effectively a series fed phased array. For multiple beams, beam scanning can also be achieved by optimizing the coupling parameters once and then fixing them while changing the phase shift values. To demonstrate this, we chose to divide a scanning range of $[-60°, 60°]$ into three regions $[-60°, -20°]$, $[-20°, 20°]$, and $[20°, 60°]$, and produce three scanning beams in the three regions.

To investigate the optimality of the above strategy, we first optimize the Blass-like GJC matrix to produce three beams pointing at $(-30°, 0°$ and $30°)$. Then, we scan the three beams by simply changing the phase shifter values according to (19). The results are shown in Fig. 10. It is seen that the

TABLE I: Magnitudes of array excitation vector elements for N = 8 and M = 3. Achieved $\eta_t = 95.8\%$.

	Ant1	Ant2	Ant3	Ant4	Ant5	Ant6	Ant7	Ant8
Beam1	0.3536	0.3536	0.3536	0.3536	0.3536	0.3536	0.3536	0.3536
Beam2	0.3536	0.3536	0.3536	0.3536	0.3636	0.3536	0.3536	0.1831
Beam3	0.3536	0.3515	0.3536	0.3536	0.3536	0.3435	0.3310	0.3243

TABLE II: Magnitudes of array excitation vector elements for N = 12 and M = 3. Achieved $\eta_t = 97.0\%$.

	Ant1	Ant2	Ant3	Ant4	Ant5	Ant6	Ant7	Ant8	Ant 9	Ant10	Ant11	Ant12
Beam1	0.2887	0.2887	0.2887	0.2887	0.2887	0.2887	0.2887	0.2887	0.2887	0.2887	0.2887	0.2887
Beam2	0.2887	0.2887	0.2887	0.2887	0.2887	0.2887	0.2887	0.2887	0.2887	0.2887	0.2887	0.1534
Beam3	0.2887	0.2887	0.2887	0.2887	0.2887	0.2887	0.2887	0.2887	0.2887	0.2887	0.2696	0.2530

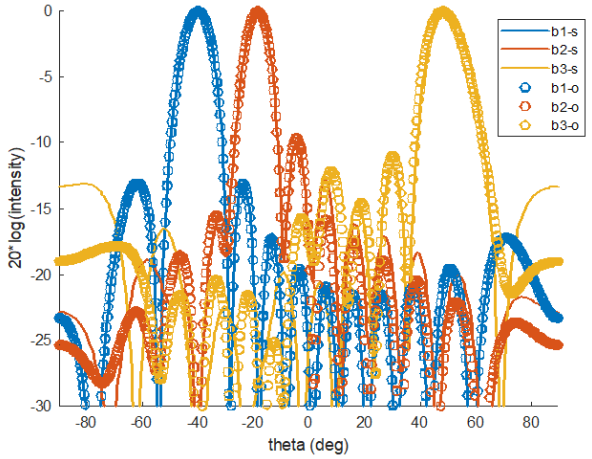

Fig. 10: Multiple beam scanning by changing phase shifts only (solid line, -s), and optimizing the GJC matrix (circles, -o) with M=3, N = 12.

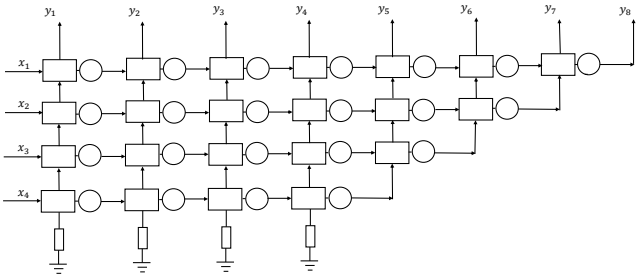

Fig. 11: Illustration of a 4×8 Nolen-like GJC Matrix.

beam patterns are well maintained. This is significant as it means that Blass-like GJC matrices can be used for *multibeam phased arrays*. To further confirm this, Fig. 10 also compares the beams pointing at $(-40°, -20°, 50°)$ produced by direct optimization of the directional couplers and by just changing the phase shift values, respectively. It is observed that the two sets of results are highly similar. It should be noted that the sidelobe levels of the second and third beams from the left have higher sidelobes than the first. To prevent beams associated with the lower beam ports from deteriorating, in practice, the number of antenna elements N would need to be sufficiently high compared with the number of beams M.

C. Nolen-like GJC Matrix

For clarity, we have investigated only Blass-like matrices with N columns and M rows so far. A generalized joined coupler (GJC) matrix doesn't need to be a full rectangular matrix. Depending on the specific performance and cost requirements, some elements can be removed. The GJC can be terminated by match loads, or similar to the Nolen matrix, one can truncate some rows and direct the signal flow in the last nodes upwards. This results in a lossless Nolen-like GJC matrix shown in Fig.11.

In fact, a Nolen matrix is realized by setting the parameters of the diagonal directional couplers as $\theta_{m(N-m+1)} = \pi/2$, $m = 1, 2, \cdots, M$, thus preventing the signal flow from passing from left-to-right through the directional couplers positioned along the diagonal of the Nolen matrix. Since all the input energy to an ideal Nolen matrix is directed to the antenna elements, Nolen matrices are understood to be lossless and thus have been recently favored for implementation. The synthesis of Nolen matrices can be realized using the theory developed in Section II; One simply needs to have the parameters of the diagonal couplers fixed to $\pi/2$. The prameters of matrix nodes below the diagonal ones can be set to any values as they do not affect the calculations and would effectively not exist in the physical implementation of this matrix.

Although the Nolen matrix is lossless and requires almost only half of the elements of the Blass matrix for large N, it does exhibit critical drawbacks; to produce N beams with a Nolen matrix, we have $N-1$ variables to optimize Beam 1, $N-2$ variables to produce Beam 2, and so on. We do not have any variable to optimize beam N. Effectively, beam N is determined by the $N-1$ beams. The quality of the higher order beams can thus deteriorate significantly. To show this,

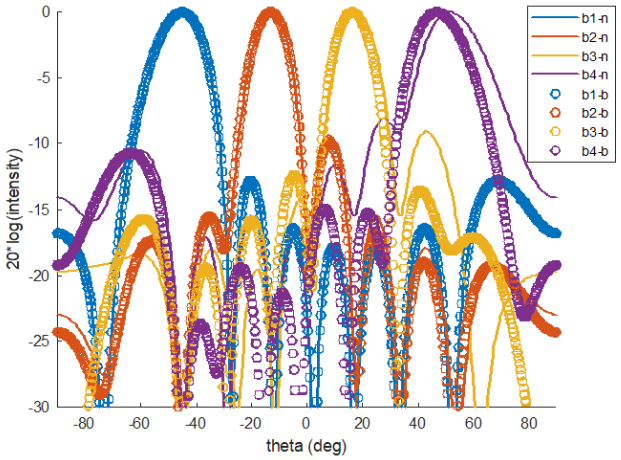

Fig. 12: Comparison of four beams produced by a Blass-like GJC matrix (circles, -b) and a Nolen-like GJC matrix (solid line, -n) using eight antenna elements (M=4, N = 8).

we chose a Nolen-like GJC matrix with $N = 8$ and $M = 4$, and set the parameters of the last four diagonal elements as $\theta_{m(N-m+1)} = \pi/2,\ m = 1,\ 2,\ 3,\ 4$. We call it a Nolen-like GJC matrix as it is not diagonal, and its configuration is shown in Fig. 11. Some numerical results of the Nolen-like GJC matrix are provided in Fig. 12. The matched loads at the bottom of the matrix are for receiving only, and they do not consume any transmission power. It is seen from Fig. 12 that, compared with the Blass-like GJC matrix counterparts, the 3^{rd} and 4^{th} beams produced by the Nolen-like GJC matrix have more prominent sidelobes in addition to broadened main lobes as a result of reduced matrix nodes.

As stated earlier, a GJC matrix can take many forms, and there are many issues to be investigated further using the approach presented above. This is the topic of our on-going study.

V. Conclusions

Analogue multiple beamforming serves as a low-cost and energy efficient way to produce multiple beams. The Blass matrix is usually regarded as too lossy, and, therefore, recent research activities have been focused on the Nolen matrix. To address the issue of lacking general theory and synthesis approaches, we have developed a new theory for synthesizing multiple beams with individual beam direction and sidelobe control using the generalized joined coupler (GJC) matrix, and have shown how the proposed approach can be employed through numerical examples. We demonstrated that the loss of a Blass-like GJC matrix can be made relatively small and therefore it would deserve more attention as a candidate for feeding multibeam antenna arrays. The Nolen matrix and the Nolen-like GJC matrices may lead to faster beam quality degradation than in the Blass-like GJC matrix case if many beams are needed. We have also shown that low sidelobe multibeam phased arrays can be produced by using appropriate distribution functions as the optimization target, and using tuneable phase shifters to control the beam directions. It is expected that the theory presented and the features of the Blass-like GJC matrices and Nolen-like matrices revealed will facilitate future research and adoption of circuit-type multiple beamforming networks.

References

[1] Y. J. Guo, M. Ansari, and N. J. G. Fonseca, "Circuit type multiple beamforming networks for antenna arrays in 5g and 6g terrestrial and non-terrestrial networks," *IEEE Journal of Microwaves*, vol. 1, no. 3, pp. 704–722, 2021.

[2] W. Hong and *et al.*, "Multibeam antenna technologies for 5g wireless communications," *IEEE Transactions on Antennas and Propagation*, vol. 65, p. 6231–6249, 2017.

[3] W. Roh, J. Y. Seol, J. Park, B. Lee, J. Lee, Y. Kim, J. Cho, K. Cheun, and F. Aryanfar, "Millimeter-wave beamforming as an enabling technology for 5g cellular communications: Theoretical feasibility and prototype results," *IEEE Communications Magazine*, vol. 52, no. 2, p. 106–113, 2014.

[4] Y. Aslan, A. Roederer, N. J. G. Fonseca, P. Angeletti, and A. Yarovoy, "Orthogonal versus zero-forced beamforming in multibeam antenna systems: Review and challenges for future wireless networks," *IEEE Journal of Microwaves*, vol. 1, p. 879–901, 2021.

[5] Y. J. Guo, M. Ansari, R. W. Zilkowski, and N. J. G. Fonseca, "Quasi-optical multi-beam antenna technologies for b5g and 6g mmwave and thz networks: A review," *IEEE Open Journal of Antennas and Propagation*, vol. 2, pp. 807–830, 2021.

[6] J. Butler, "Beam-forming matrix simplifies design of electronically scanned antenna," *Electronic Design*, vol. 9, p. 170–173, 1961.

[7] H. Moody, "The systematic design of the butler matrix," *IEEE Transactions on Antennas and Propagation*, vol. 12, no. 6, pp. 786–788, 1964.

[8] H. Zhu and Y. J. Guo, "Wideband dual-beam-forming antenna arrays," *IEEE Transactions on Antennas and Propagation*, vol. 67, pp. 1590–1604, 2019.

[9] J. Blass, "Multidirectional antenna - a new approach to stacked beams," *IRE International Convention Record*, pp. 48–50, 1960.

[10] J. Nolen, "Synthesis of multiple beam networks for arbitrary illuminations," *Ph.D. dissertation, Radio Div., Bendix Corp., Baltimore, MD, USA*, 1965.

[11] W. P. DELANEY, "An rf multiple beam-forming technique," *IRE TRANSACTIONS ON MILITARY ELECTRONICS*, vol. 6, pp. 179–186, 1962.

[12] W. R. Jones and E. C. DuFort, "On the design of optimum dual-series networks," *IEEE Transactions on Microwave Theory and Technology*, vol. MTT-19, pp. 151–158, 1971.

[13] N. J. G. Fonseca, "Printed s-band 4x4 nolen matrix for multiple beam antenna applications," *IEEE Trans. Antennas Propag.*, vol. 57, no. 6, p. 1673–1678, 2009.

[14] S. Mosca, F. Bilotti, A. Toscano, and L. Vegni, "A novel design method for blass matrix beam-forming networks," *IEEE Transactions on Antennas and Propagation*, vol. 50, pp. 225–232, 2002.

[15] F. Casini, R. V. Gatti, L. Marcaccioli, and R. Sorrentino, "A novel design method for blass matrix beam-forming networks," *Proceedings of the 4th European Radar Conference*, pp. 232–235, 2007.

[16] H. Ren, H. Zhang, Y. Jin, Y. Gu, and B. Arigong, "A novel 2-d 3×3 nolen matrix for 2-d beamforming application," *IEEE Transactions on Microwave Theory and Techniques*, vol. 67, no. 11, pp. 4622–4631, 2019.

[17] T. Djerafi, N. J. G. Fonseca, and K. Wu, "Planar ku-band 4 x 4 nolen matrix in siw technology," *IEEE Trans. Microw. Theory Tech.*, vol. 58, no. 2, pp. 259–266, 2010.

[18] C. Tsokos and *et al.*, "Analysis of a multibeam optical beamforming network based on blass matrix architecture," *Journal of Lightwave Technology*, vol. 36, no. 16, pp. 3354–3372, 2018.

[19] P. Li, H. Ren, and B. Arigong, "A symmetric beam-phased array fed by a nolen matrix using 180°couplers," *IEEE Microwave and Wireless Component Letters*, vol. 30, no. 4, pp. 387–390, 2020.

[20] R. L. Haupt, *Antenna Arrays*. John Wiley and Sons, 2010.

[21] R. E. Collin, *Foundations for Microwave Engineering, International Edition*. McGraw-Hill Inc., 1992.

[22] Y. J. Guo and R. W. Ziolkowski, *Advanced Antenna Array Engineering for 6G and Beyond Wireless Communications*. IEEE Press/Wiley, October 2021.

[23] D. W. Boeringer and D. H. Werner, "A comparison of particle swarm optimization and genetic algorithms for a phased array synthesis problem," *IEEE Antennas and Propagation Society Symposium Digest*, pp. 22–27, 2003.

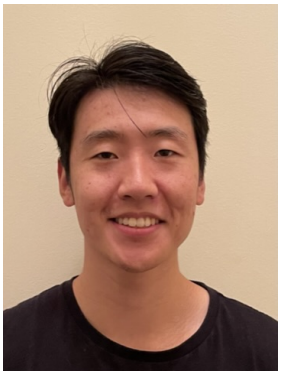

Charles A. Guo received his MRes in Physics from the University of New South Wales in 2021, and Bachelor in Science (Honours) from the University of Sydney in 2018. He is currently pursuing a Ph.D. degree in the School of Electrical and Telecommunications Engineering, University of New South Wales, New South Wales, Australia. He has been employed as a part-time Research Fellow at the University of Technology Sydney since 2018.

Charles' current research interest include artificial intelligence, signal and image processing, Internet of Things (IoT) and digital twin.

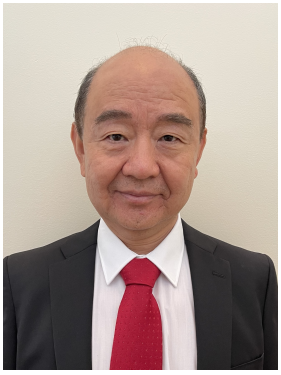

Y. Jay Guo (Fellow'2014) received a Bachelor's Degree and a Master's Degree from Xidian University in 1982 and 1984, respectively, and a Ph.D Degree from Xian Jiaotong University in 1987, all in China. His research interests include antennas, mm-wave and THz communications and sensing systems as well as big data technologies. He has published four books and over 600 research papers including over 280 IEEE Transactions papers, and he holds 26 international patents. He is a Fellow of the Australian Academy of Engineering and Technology, a Fellow of IEEE and a Fellow of IET, and was a member of the College of Experts of Australian Research Council (ARC, 2016-2018). He has won a number of the most prestigious Australian national awards including the Engineering Excellence Awards (2007, 2012) and CSIRO Chairman's Medal (2007, 2012). He was named one of the most influential engineers in Australia in 2014 and 2015, and one of the top researchers across all fields in Australia in 2020 and 2021, respectively.

He is a Distinguished Professor and the Director of Global Big Data Technologies Centre (GBDTC) at the University of Technology Sydney (UTS), Australia. He is the founding Technical Director of the New South Wales Connectivity Innovation Network. Prior to joining UTS in 2014, he served as a Director in CSIRO for over nine years. Before joining CSIRO, he held various senior technology leadership positions in Fujitsu, Siemens and NEC in the U.K.

Prof Guo has chaired numerous international conferences and served as a guest editor for a number of IEEE publications. He was the Chair of International Steering Committee, International Symposium on Antennas and Propagation (2019-2021). He has been the International Advisory Committee Chair of IEEE VTC2017, General Chair of ISAP2022, ISAP2015, iWAT2014 and WPMC'2014, and TPC Chair of 2010 IEEE WCNC, and 2012 and 2007 IEEE ISCIT. He served as Guest Editor of special issues on "*Low-Cost Wide-Angle Beam Scanning Antennas*", "*Antennas for Satellite Communications*" and "*Antennas and Propagation Aspects of 60-90GHz Wireless Communications*," all in IEEE Transactions on Antennas and Propagation, Special Issue on "*Communications Challenges and Dynamics for Unmanned Autonomous Vehicles*," IEEE Journal on Selected Areas in Communications (JSAC), and Special Issue on "*5G for Mission Critical Machine Communications*", IEEE Network Magazine.